A Fundamentals of Density Functional Theory

A.1 The Kohn-Sham formulation of Density Functional Theory

The *raison d'etre* of Density Functional Theory (DFT) is the solution of the many-body Hamiltonian for a system of N electrons and M positively-charged nuclei (or ions) in a crystalline solid, the starting point for nearly all problems in solid-state physics. Neglecting all relativistic and magnetic effects, this Hamiltonian can be written as:

$$\begin{aligned}\widehat{H_N} = &-\frac{\hbar^2}{2m_e}\sum_{i=1}^{N}\nabla_i^2 - \sum_{i,I=1}^{N,M}\frac{Z_I e^2}{4\pi\varepsilon_0\left|\mathbf{r_i}-\mathbf{R_I}\right|} + \frac{1}{2}\sum_{i,j}^{i\neq j}\frac{e^2}{4\pi\varepsilon_0\left|\mathbf{r_i}-\mathbf{r_j}\right|} \\ &-\sum_{I=1}^{M}\frac{\hbar^2}{2M_I}\nabla_I^2 + \frac{1}{2}\sum_{I,J}^{I\neq J}\frac{Z_I Z_J e^2}{4\pi\varepsilon_0\left|\mathbf{R_I}-\mathbf{R_J}\right|}\end{aligned} \tag{23}$$

where the electrons are denoted by lower case subscripts and the nuclei, with charge Z_I and mass M_I, by upper case subscripts. The terms in this Hamiltonian represent, from left to right, the kinetic energy of the electrons, the attractive potential acting on the electrons due to the nuclei, the repulsive electron-electron interaction, the kinetic energy of the nuclei and finally the repulsive internuclear electrostatic interaction. In practice, such an elementary equation as Eq. 23 is impossible to solve analytically for all but the most trivial systems because of the enormously complicating effects of the interactions between electrons, which leads to coupling between the electronic coordinates in the system. This coupling manifests itself under the well-known phenomena of inter-electron exchange and correlation interactions in Quantum Mechanics . The issue central to the theory of electronic structure is therefore the development of approximate methods using simplifying physical ideas to treat electronic interactions and correlations with sufficient accuracy such that, starting from Eq. 23, one can still gain insight into the diverse array of electronic properties and phenomena exhibited by real solid matter.

One initial simple approximation involves setting the mass of the ions M_I to infinity, which is tantamount to saying that the positions of the ions are assumed fixed to their corresponding lattice points within the crystal structure. This so-called Born-Oppenheimer, or Adiabatic, approximation in electronic structure calculations allows the ionic kinetic energy term in Eq, 23 to be ignored, which is an excellent approximation for most intent and purposes. Neglecting also the final inter-ionic electrostatic interaction term, which is essential in total energy calculations but reduces to a simple classical additive term within the Born-Oppenheimer approximation, the initial problem of solving the electronic structure for the entire crystalline solid is consequently simplified to the treatment of the crystal electron cloud exclusively. The corresponding N-electron Schroedinger equation can be rewritten as:

$$\begin{aligned}&\left[\sum_{i=1}^{N}\left(-\frac{\hbar}{2m_e}\nabla_i^2 + V_{ion}\left(\mathbf{r_i}\right)\right) + \frac{1}{2}\sum_{i,j}^{i\neq j}\frac{e^2}{4\pi\varepsilon_0|\mathbf{r_i}-\mathbf{r_j}|}\right]\Psi_N\left(\mathbf{r_1},\sigma_1;\mathbf{r_2},\sigma_2;....\mathbf{r_N},\sigma_N\right) \\ &= E_N\Psi_N\left(\mathbf{r_1},\sigma_1;\mathbf{r_2},\sigma_2;....\mathbf{r_N},\sigma_N\right)\end{aligned} \tag{24}$$

where $V_{ion}(\mathbf{r_i}) = -\sum\limits_{I=1}^{M} \frac{Z_I e^2}{4\pi\epsilon_0 |\mathbf{r_i} - \mathbf{R_I}|}$ represents the combined ionic potential acting on each electron, E_N is the total electronic energy and $\Psi_N\left(r_1, \sigma_1; r_2, \sigma_2; ....r_N, \sigma_N\right)$ is the N-electron wavefunction expressed in terms of the spatial $(\mathbf{r_i})$ and spin (σ_i) quantum numbers for the i^{th} electron in the material.

Historically, an important milestone for going beyond the independent-electron approximation, embodied by the Sommerfeld free-electron model, and incorporating approximately the effect of inter-electron interactions in solids was the development of the Hartree-Fock equations [8]. Even though they were the first technique which allowed for a neat separation between electron exchange and correlation effects, in practice their treatment remains difficult and requires careful further approximations. The need for more accurate, widely-applicable and easy-to-implement methods for calculating the ground state properties of many-body molecules and solid-state systems from first-principles, or "ab-initio", while still accounting for the effects of inter-electron exchange and correlation interactions, provided an incentive for P. Hohenberg and W. Kohn to conceive the current modern formulation of DFT in 1964 [47]. In this pioneering work, the authors demonstrated that the density $n(\mathbf{r})$ of particles in the ground state of a quantum many-body system can be assigned a special role and considered as a "fundamental" variable, and that all properties of the system under investigation, including the effects of interactions and correlations among the particles, can be considered to be unique *functionals* [9] of this fundamental quantity. It follows from this crucial conjecture that the ground state electron density can be used as an effective replacement for the ground state many-body wavefunction $\Psi_G\left(r_1, \sigma_1; r_2, \sigma_2; ....r_N, \sigma_N\right)$ appearing in Eq. 24, thus significantly simplifying the scale and complexity of the problem from the full $3N$ degrees of freedom for N electrons embodied by Ψ_G. This change of variables can be expressed conceptually as follows:

$$\Psi_G = \Psi\left(\mathbf{r_1}, \sigma_1; .....; \mathbf{r_i}, \sigma_i; ......; \mathbf{r_N}, \sigma_N\right) \overset{DFT}{\longrightarrow} n\left(\mathbf{r}\right) = \left\langle \Psi_G \,\middle|\, \sum_{i=1}^{N} \delta\left(\mathbf{r} - \mathbf{r_i}\right) \Psi_G \right\rangle \tag{25}$$

This reformulation of the many-body problem is encapsulated by two cardinal theorems, known as Hohenberg-Kohn (HK) theorems, which together establish the theoretical foundations of all modern formulations of DFT. Apart from encompassing the important role assigned to the ground state density in DFT mentioned previously, the HK theorems also provide insight in the relation between the ground state density of a system of mutually-interacting electrons and any general external potential $V_{ext}\left(\mathbf{r}\right)$ acting upon it (for example, the Coulomb potential due to the nuclei in the periodic crystal structure of a material). The HK theorems, which will be stated here without proof [10], can be expressed as follows:

1. **Theorem 1**: For any system of interacting particles bathed in an external potential $V_{ext}\left(\mathbf{r}\right)$, the potential $V_{ext}\left(\mathbf{r}\right)$ is determined uniquely, except for

---

[8] For an introduction to the mathematical formalism of Hartree-Fock theory, see for example page 332 in Ref. [5].

[9] Familiarity with the mathematical concept of Functional is assumed in this report. For an introduction to the theory of Funcionals and their applications in Calculus of Variations, the reader is referred to Chapt. 22 in Ref [98].

[10] For a formal proof of the HK theorems, consult for example section 6.2 in Ref. [71].

$$\begin{tikzcd}
V_{\mathrm{ext}}(\mathbf{r}) \arrow[d, Rightarrow] & n_0(\mathbf{r}) \arrow[l, Rightarrow, "\mathrm{HK}"'] \\
\Psi_i(\{\mathbf{r}\}) \arrow[r, Rightarrow] & \Psi_0(\{\mathbf{r}\}) \arrow[u, Rightarrow]
\end{tikzcd}$$

Figure 28: Flow diagram illustrating the one-to-one correspondence between the external potential $V_{ext}\left(\mathbf{r}\right)$ acting on the system of interacting electrons, its ground state density $n_o(\mathbf{r})$ and its set of eigenstates $\Psi_i\left(\{\mathbf{r}\}\right)$, as demonstrated by the first HK theorem. (Figure reproduced from Ref. [71])

   a constant, by the ground state particle density $n_o(\mathbf{r})$.
   Corollary 1: Since the hamiltonian of the system is thus fully determined, except for a constant shift of the energy, it follows that the many-body wavefunctions for all states (ground and excited), and consequently all internal properties of the system, are completely determined from the solution of the corresponding Schroedinger Equation given only the ground state density.

2. **Theorem 2**: Any internal property of the system, including its total energy, can be expressed as a unique functional of the density $n(\mathbf{r})$, valid for any external potential $V_{ext}\left(\mathbf{r}\right)$. For any particular $V_{ext}\left(\mathbf{r}\right)$ the exact ground state energy of the system is the global minimum value of the functional of the total energy $E[n]$, and the density $n(\mathbf{r})$ that minimizes the functional is the exact ground state density $n_o(\mathbf{r})$.
   Corollary 2: The functional $E[n]$ alone is sufficient to determine only the exact ground state energy and density. In general, excited states of the electrons must be determined by other means.

The logic behind the HK theorems is summarized schematically in Fig 28. The challenge posed by the Hohenberg-Kohn theorems is how to make use of the reformulation of many-body theory in terms of functionals of the density. Such a functional for the total ground-state energy of the system can be written in general as:

$$E_N\left[n(\mathbf{r})\right] = T_S\left[n(\mathbf{r})\right] + E_{Hartree}\left[n(\mathbf{r})\right] + E_{XC}\left[n(\mathbf{r})\right] + \int d^3\mathbf{r}V_{ext}(\mathbf{r})n(\mathbf{r}) + E_{II} \tag{26}$$

where E_{II} is the interaction energy of the nuclei among themselves, and $T[n]$, $E_{Hartree}[n]$ and $E_{XC}[n]$ represent respectively the kinetic, classical Coulomb interaction (Hartree) and Exchange-Correlation energies of the electron cloud, all of which are internal properties of the electron system and are therefore expressible as functionals of the density according to the second HK theorem. At this stage however we are still left with the problem of finding explicit forms

$$\begin{tikzcd}
V_{ext}(\mathbf{r}) \arrow[d, Rightarrow] & n_0(\mathbf{r}) \arrow[l, Rightarrow, "HK"'] \arrow[r, Leftrightarrow, "KS"] & n_0(\mathbf{r}) \arrow[r, Rightarrow, "HK_0"] & V_{KS}(\mathbf{r}) \arrow[d, Rightarrow] \\
\Psi_i(\{\mathbf{r}\}) \arrow[r, Rightarrow] & \Psi_0(\{\mathbf{r}\}) \arrow[u, Rightarrow] & \psi_{i=1,N_e}(\mathbf{r}) \arrow[u, Rightarrow] & \psi_i(\mathbf{r}) \arrow[l, Rightarrow]
\end{tikzcd}$$

Figure 29: Schematic representation of the KS ansatz. The label "HK_o" denotes the HK theorem applied to the non-interacting auxiliary system of electrons. The connection in both directions between the two systems is established by the arrow labeled "KS", showing that in principle solution of the independent-particle KS problem determines all properties of the original interacting system. (Figure reproduced from Ref. [71])

for the constituent functionals in Eq. 26. While on one hand there exists a simple expression linking the Hartree potential energy to the density:

$$E_{Hartree}\left[n\right] = \frac{1}{2}\int d^3\mathbf{r}d^3\mathbf{r}'\frac{n\left(\mathbf{r}\right)n\left(\mathbf{r}'\right)}{4\pi\epsilon_0\left|\mathbf{r}-\mathbf{r}'\right|} \tag{27}$$

this task is more problematic for the Kinetic energy term $T[n]$, for which there is no known direct connection to the density, and for the Exchange-Correlation energy functional $E_{XC}[n] = E_X[n]+E_C[n]$ incorporating all the complex many-body exchange ($E_X[n]$) and correlation ($E_C[n]$) effects, which cannot be modeled analytically.

A significant step forward from this impasse was accomplished by the seminal work performed in 1965 by W. Kohn and L.J. Sham [63], which lead to the now well-established Kohn-Sham (KS) approach to DFT . The defining *Ansatz* of the KS formulation of DFT was to map the difficult interacting many-body system obeying the Hamiltonian of Eq. 24 to a different fictitious auxiliary system of non-interacting particles that can be solved more easily, with the condition that its ground state density be equal to that of the original interacting system and consequently that its internal physical properties be equivalent. This leads to the relation between the actual and auxiliary systems depicted in Fig. 29. Even though it has never been proven formally that this auxiliary system is capable of reproducing precisely all the physical properties of the original interacting problem, this basic assumption yields excellent approximations for the problems of greatest practical interest, and in particular for ground-state calculations which are by far the most widespread applications of DFT. Solution of the KS auxiliary system for the ground state can be viewed as the problem of minimization of the total ground state energy functional of Eq. 26 with respect to small variations in the density $\delta(n(\mathbf{r},\sigma))$. One of the major qualities of the KS approach is that it allows the electronic density of the indepent-particle auxiliary system to be expressed as a simple sum of the probability densities associated with each single-particle wavefunction $\psi_i^\sigma(\mathbf{r})$:

$$n\left(\mathbf{r}\right) = \sum_\sigma n(\mathbf{r},\sigma) = \sum_\sigma\sum_{i=1}^{N^\sigma}\left|\psi_i^\sigma\left(\mathbf{r}\right)\right|^2 \tag{28}$$

The establishment of such a relation between density and wavefunctions allows in turn the functional for the kinetic energy in Eq. 26 to be kept expressed in terms of the single-particle orbitals, without therefore the need to find an explicit dependence on the density:

$$T_s = -\frac{\hbar^2}{2m_e}\sum_{\sigma}\sum_{i=1}^{N^\sigma}\left\langle\psi_i^\sigma \mid \nabla^2\psi_i^\sigma\right\rangle = -\frac{\hbar^2}{2m_e}\sum_{\sigma}\sum_{i=1}^{N^\sigma}|\nabla\psi_i^\sigma|^2 \tag{29}$$

Given that all other functionals of the density in Eq. 26 can now also be expressed in terms of the independent-particle orbitals $\psi_i^\sigma(\mathbf{r})$ via Eq. 28, the problem of minimizing Eq. 26 to find the ground-state energy of the system can be reformulated in terms of variations of the orbitals via the chain rule, which yields the following variational equation:

$$\frac{\delta E_N}{\delta\psi_i^{\sigma *}(\mathbf{r})} = \frac{\delta T_S}{\delta\psi_i^{\sigma *}(\mathbf{r})} + \left[\frac{\delta E_{ext}}{\delta n(\mathbf{r},\sigma)} + \frac{\delta E_{Hartree}}{\delta n(\mathbf{r},\sigma)} + \frac{\delta E_{XC}}{\delta n(\mathbf{r},\sigma)}\right]\frac{\delta n(\mathbf{r},\sigma)}{\delta\psi_i^{\sigma *}(\mathbf{r})} = 0 \tag{30}$$

subject to the orthonomalization constraint on each of the single-particle orbitals:

$$\left\langle\psi_i^\sigma \;\middle|\; \psi_j^{\sigma'}\right\rangle = \delta_{i,j}\delta_{\sigma,\sigma'} \tag{31}$$

Using expressions 29 and 28 for calculating the derivatives involving the Kinetic Energy and the density:

$$\frac{\delta T_S}{\delta\psi_i^{\sigma *}(\mathbf{r})} = -\frac{1}{2}\nabla^2\psi_i^\sigma(\mathbf{r});\; \frac{\delta n^\sigma(\mathbf{r})}{\delta\psi_i^{\sigma *}(\mathbf{r})} = \psi_i^\sigma(\mathbf{r}) \tag{32}$$

and the Lagrange multiplier method for constrained minimization [11], we obtain the following set of Schroedinger-like equations, one for each of the N single-particle orbitals in the auxiliary system:

$$\begin{gathered}\left(H_{KS}^\sigma - \varepsilon_i^\sigma\right)\psi_i^\sigma(\mathbf{r}) = 0 \\ \{\psi_i^\sigma : i = 1, N\}\end{gathered} \tag{33}$$

where the Lagrange parameters ϵ_i represent the possible eigenvalues. It is important to stress that these eigenvalues do not correspond to the single-particle energies as in a normal Schroedinger Equation, and in fact have no obvious physical meaning except for the highest one, which corresponds to the ionization energy of the system. H_{KS} on the other hand represents the effective KS Hamiltonian:

$$\begin{aligned}&H_{KS}^\sigma(\mathbf{r}) = -\frac{\hbar^2}{2m_e}\nabla^2 + V_{KS}^\sigma(\mathbf{r}) \\ &\text{where } V_{KS}^\sigma(\mathbf{r}) = \frac{\delta E_{ext}}{\delta n(\mathbf{r},\sigma)} + \frac{\delta E_{Hartree}}{\delta n(\mathbf{r},\sigma)} + \frac{\delta E_{XC}}{\delta n(\mathbf{r},\sigma)} = V_{ext}^\sigma(\mathbf{r}) + V_{_{Hartree}}^\sigma(\mathbf{r}) + V_{_{XC}}^\sigma(\mathbf{r})\end{aligned} \tag{34}$$

Equations 33 and 34, collectively referred to as the *Kohn-Sham equations*, represent the culminating point of the entire KS formulation of DFT. By diagonalizing and solving the equations self-consistently (in practice by numerical means) one can first compute all the single-particle KS eigenstates $\psi_i^\sigma(\mathbf{r})$, and from there the ground-state density and total ground-state energy of the original

---

[11] An introduction to this mathematical technique is provided in section 5.9 in Ref. [98]

interacting system from Equations 28 and 26 respectively, with an accuracy limited only by the approximations in the exchange-correlation functional (given that all other functionals in Eq. 26 can be computed exactly within the KS approach) . In fact, the development and availability today of highly accurate exchange-correlation functionals with a broad range of applications has been the determining factor for elevating DFT to its current position as the most accurate, computationally-efficient and widely used technique for ab-initio electronic structure calculations in a wide range of atoms, molecules and condensed matter systems. The next section in this document is devoted to the description of the approximations for this functional most entrenched in the Condensed-Matter Physics community.

A.2 The Local Density and Generalized Gradient approximations for the exchange-correlation energy functional

Already in their seminal paper [63], Kohn and Sham pointed out that solids can often be considered as close to the limit of the homogeneous electron gas. In this limit, it is known that the effects of exchange and correlation are rather local in character, and they proposed making the local density approximation (LDA) (or more generally the local spin density approximation (LSDA), which accounts also for the spins of the electrons in a spin-polarized system) in which the exchange-correlation energy is simply an integral over all space, with the exchange-correlation energy density $\epsilon_{XC}([n], \mathbf{r})$ at each point $\mathbf{r}$ assumed to be the same as in a homogeneous electron gas of interacting electrons with the same local density:

$$E_{XC}^{LDA}[n] = \int d^3\mathbf{r} n(\mathbf{r}) \varepsilon_{XC}^{\mathrm{hom}}\left(n(\mathbf{r})\right) = \int d^3\mathbf{r} n(\mathbf{r}) \left[\varepsilon_{X}^{\mathrm{hom}}\left(n(\mathbf{r})\right) + \varepsilon_{C}^{\mathrm{hom}}\left(n(\mathbf{r})\right)\right] \tag{35}$$

The corresponding exchange-correlation potential appearing in the KS equations is consequently given by:

$$V_{XC}^{\sigma}(\mathbf{r}) = \frac{\delta E_{XC}^{LDA}[n]}{\delta n(\mathbf{r}, \sigma)} = \left[\varepsilon_{XC}^{\mathrm{hom}} + n \frac{\partial \varepsilon_{XC}^{\mathrm{hom}}}{\partial n^{\sigma}}\right]_{\mathbf{r},\sigma} \tag{36}$$

The only information needed within the LDA approximation is therefore the exchange-correlation energy of the homogeneous gas as a function of density. Since the exchange energy of an homogeneous electron gas can be calculated analytically within Hartree-Fock theory, and is given by [12]:

$$\varepsilon_{X}^{\mathrm{hom}} = -\frac{3}{4} \frac{e^2 k_F}{\pi} = -\frac{3e^2}{4\pi a_o} \left(k_F a_o\right) \tag{37}$$

where k_F is the Fermi wavevector and a_o the Bohr Radius, the LDA simply boils down to fitting numerical correlation energies for the homogeneous gas, for example by Monte Carlo total energy calculations [91, 14]. A variety of LDA expressions for the correlation energy have been proposed with time, and the most celebrated are summarized in Appendix B of Ref. [71]. The LDA

---

[12] A derivation of this expression can be found in Chapt. 17 of Ref. [5].

is expected to give the best results for solids close to a homogeneous electron gas in which the charge density is slowly varying (like a nearly-free-electron metal) and worst for very inhomogeneous cases, like for the case of atoms where the density must go continuously to zero outside the atom, or indeed in any general covalently-bound solid. However, experience has proved the LDA to be a surprisingly good approximation for a wide variety of solid-state systems.

The remarkable success of the LDA in most applications has stimulated ideas for the development of various Generalized Gradient Approximations (GGAs) [87, 88, 90], with marked improvement over LDA in many cases. The first step beyond the local approximation was the introduction of a functional of the magnitude of the density gradient $|\nabla n^{\sigma}(\mathbf{r})|$ in addition to the value of $n(\mathbf{r})$ at each point $\mathbf{r}$, which lead to the so-called Gradient Expansion Approximation (GEA). However, the GEA was found to often yield worse results than the LDA due to the large density gradients found in real materials, which cause the expansion to break down. The GGA provided the solution by introducing functions that modify the behavior at large gradients in such a way as to preserve the desired properties of the material under investigation. Within the the context of the GGA, it is convenient to generalize the expression for the Exchange-correlation functional given by Eq. 35 to include explicitly the dependence on the various orders of the density gradient $|\nabla^m n^{\sigma}(\mathbf{r})|$:

$$\begin{aligned} E_{XC}^{GGA}[n] &= \int d^3 r n(r) \varepsilon_{XC}\left(n, |\nabla n|, \left|\nabla^2 n\right| ...... |\nabla^m n|\right) \\ &\equiv \int d^3 r n(r) \varepsilon_X^{\text{hom}}(n) F_{XC}\left(n, |\nabla n|, \left|\nabla^2 n\right| ...... |\nabla^m n|\right) \end{aligned} \tag{38}$$

where F_{XC} is a dimensionless function, known as the enhancement factor of the exchange-correlation functional, and $\epsilon_x^{hom}(n)$ is the exchange energy density of the homogeneous electron gas given by Eq. 37. An expression for the exchange-correlation potential appearing in the KS equations can also be found by calculating the change $\delta E_{XC}[n]$ to linear order in δn and $\delta \nabla n = \nabla \delta n$:

$$V_{XC}^{\sigma}(\mathbf{r}) = \frac{\delta E_{XC}^{GGA}[n]}{\delta n(\mathbf{r}, \sigma)} = \left[\varepsilon_{XC} + n\frac{\partial \varepsilon_{XC}}{\partial n^{\sigma}} - \nabla\left(n\frac{\partial \varepsilon_{XC}}{\partial \nabla n^{\sigma}}\right)\right]_{\mathbf{r},\sigma} \tag{39}$$

It is natural to work in terms of dimensionless reduced density gradients of m^{th} order that can be defined by:

$$s_m = \frac{|\nabla^m n|}{(2k_F)^m n} \tag{40}$$

With this notation, the lowest order terms in the expansion of the exchange part F_X and correlation part F_C of F_{XC} have been calculated analytically:

$$F_X = 1 + \frac{10}{81}s_1^2 + \frac{146}{2025}s_2^2 + ... \tag{41}$$

and

$$F_C = \frac{\varepsilon_C^{LDA}(n)}{\varepsilon_X^{LDA}(n)}\left(1 - 0.219 s_1^2 + ...\right) \tag{42}$$

where F_C is expressed as a correction to the corresponding LDA expressions for the exchange and correlation energy densities. One of the defining characteristics of GGAs is that they lead to an exchange energy lower than their

LDA counterparts, since $F_x \geqslant 1$. The resulting reduction of the cohesive energy improves markedly the agreement with experiment for atoms, molecules and solids, and therefore constitutes a significant step forward over the LDA overbinding [54, 23]. Numerous different forms have been proposed for the higher-order terms in the expansions for F_C and F_X by choosing different physical conditions for $s \to \infty$, leading to very different behaviors in the region of large density gradients. Hence, even if one form of GGA somehow gives the correct result for a certain physical property while others fail, the same form is not necessarily superior for other properties in which different physical conditions prevail.

A.3 Computational self-consistent solution of the Kohn-Sham equations: the plane-wave pseudopotential method

In order to solve in practice the eigenvalue problem presented by the KS equations (33), the single-particle eigenstates $\psi_i^\sigma(\mathbf{r})$ must be expanded in some orthogonal basis set. The simplest and most popular choice for this basis is to use orthogonal plane-wave functions, under the so-called orthogonalized planewave (OPW) method [101, 46, 65] . These plane-waves can be expressed as [13]:

$$\psi_{\mathbf{k}}^i(\mathbf{r}) = \sum_{\mathbf{G}} c_{\mathbf{k}}^n(\mathbf{G}) e^{i(\mathbf{k}+\mathbf{G})\cdot\mathbf{r}} \tag{43}$$

where $\mathbf{k}$ is the crystal momentum and the sum is over all Bravais lattice vectors $\mathbf{G}$ of the reciprocal lattice of the system under investigation. This discrete basis set can in theory be made infinite in size by application of periodic boundary conditions to the problem, but in practice a finite number of plane-wave basis states is normally sufficient to converge systematically most physical quantities of interest in typical computational problems. As explained in Fig. 30, in order to truncate the basis set, the sum term in Eq. (43) is limited to a set of reciprocal lattice vectors encompassed by a sphere with radius defined by the cutoff kinetic energy, E_{cut}:

$$\frac{\hbar^2 \left|\mathbf{k}^2 + \mathbf{G}^2\right|}{2m} \leqslant E_{cut} \tag{44}$$

so that the entire set of plane-waves can be defined by this maximum kinetic energy component. More recently, the OPW method has been reformulated and adapted to modern techniques for calculation of total energy, forces and stress under the so-callled Projector-Augmented Wave (PAW) method [9], which introduces projectors and auxiliary localized functions for a more efficient solution of the KS eigenvalue problem.

The choice of plane waves as basis set however requires to be operated in conjunction with the implementation of pseudopotentials [19, 93, 20] in order to limit the size of this expansion to computationally-feasible proportions for the solution of realistic systems. Pseudopotentials allow for a neat separation between the treatment of core electrons in an atom, that is those electrons which are tightly-bound to the nucleus and are therefore not involved in the interactions between atoms, and the valence electrons, which on the other hand are more loosely bound and consequently dictate the chemical properties of the

---

[13] This form for the plane-wave functions can be shown to be the most general solution satisfying Bloch's Theorem for periodic boundary conditions in a crystal lattice.

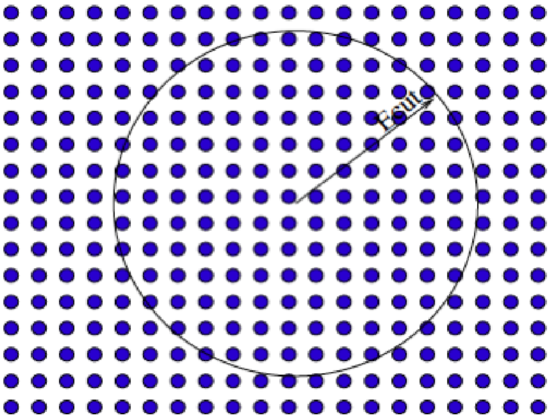

Figure 30: Truncation of the plane wave basis states expansion at a sphere of radius E_{cut} in reciprocal space. The blue dots represent the discrete reciprocal lattice vectors available for the expansion. (Figure reproduced from Ref. [92].)

material. As a direct consequence of the orthogonality requirement on the single-electron wavefunctions, the superposition of the valence and core electron wavefunctions results in a many-electron wavefunction exhibiting strong-oscillations in the region near the nucleus, as illustrated in Fig. 31. These oscillations become inevitably quite difficult to model using a plane-wave basis set, requiring many plane-waves for an accurate description. It therefore becomes convenient to ignore altogether the region in the immediate surroundings of the nucleus, and this is indeed the approach adopted by the pseudopotential approximation, where only the valence electrons of atoms are explicitly considered and the screening effects of the inner core electrons contained within the cutoff nuclear radius r_c indicated in Fig. 31 are integrated within a new effective ionic potential (the pseudopotential). The remaining smoother variation of the all-electron valence wavefunction in the outskirts of the nuclear region beyond r_c can be modeled accurately with a much more restricted size for plane-wave basis set, with the consequent sharp gain in computational efficiency. The pseudopotential approach turns out to be an excellent approximation for practical calculations since, as mentioned previously, this region remains almost completely shielded from all neighboring interactions, and the oscillations are consequently of very little consequence for the electronic structure of the solid.

When constructing a new pseudopotential, the main goals that need to be attained are threefold: firstly, the pseudodpotential should be as soft as possible, meaning that it should allow expansion of the valence pseudo-wavefunctions using as few plane-waves as possible. Secondly, it should be as transferrable as possible, in the sense that a pseudopotential generated for a given atomic configuration should accurately reproduce others. This helps to ensure that its application in solid-state systems, where the overall crystal potential is inevitably different from an atomic potential, be capable of reliable results. Finally, the pseudo-charge density, that is the charge density constructed using the pseudo-wavefunctions, should reproduce the valence charge density of the atom under consideration as accurately as possible. The concept of *norm-conservation* in

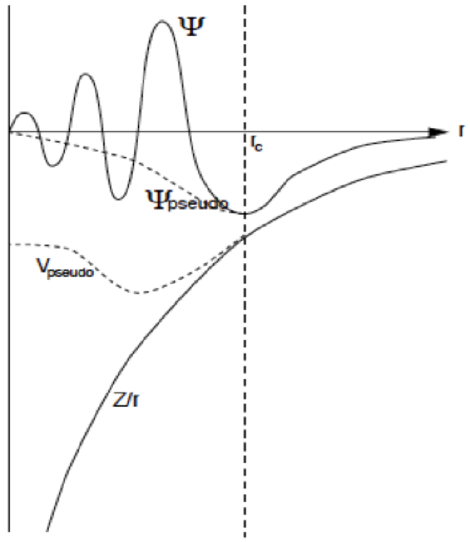

Figure 31: Schematic representation of the concept of pseudopotential. Ψ labels the true all-electron wavefunction, while Ψ_{pseudo} the all-electron pseudowavefunction which results from subsituting the true bare Coulombic nuclear potential Z/r with the modified pseudopotential V_{pseudo} incorporating the screening effects of the inner core electrons. The smooth variation of Ψ beyond the core radius r_c implies that an accurate emulation of the atomic interaction with Ψ_{pseudo} requires only a limited plane-wave basis expansion, thus making the pseudopotential a very efficient approximation for most atomic systems. (Figure reproduced from Ref. [92].)

pseudopotential theory [42] provided the first systematic solution for reconciling these conflicting goals. Within norm-conserving pseudopotentials, the pseudo-wavefunctions are designed and constructed to be equivalent to the actual valence wavefunctions outside the core radius r_c. Inside r_c on the other hand, the pseudo-wavefunctions are allowed to differ from the true wavefuntions, but their norm is constrained to be the same.

A radical departure from the concept of norm-coservation in pseudopotentials was eventually proposed by Vanderbilt and co-workers [104, 68, 67]. In this approach, which became to be known as the *ultra-soft* pseudopotential method, the pseudo-wavefunctions are required to be equal to the all-electron wavefunctions outside r_c as with norm-conserving pseudopotentials, but inside r_c they are allowed to be as soft as possible, which is accomplished by removing the norm-conservation constraint. Even though the use of non-normalized wavefunctions complicates the solution of the KS equations, this approach offers the major advantage of greatly reducing the required plane-wave cutoff without sacrificing the accuracy of the calculation, which explains its popularity for use in large-scale calculations. The computational work presented in this report was no exception.

One final aspect of the computational implementation of DFT worth mentioning is the techniques used for determining the charge density and other quantities which can be extracted from DFT calculations such as total energy and atomic forces. The evaluation of all these quantities require summations to be performed over the occupied states, which for crystals translate into integrals over the Brillouin zone. Exploiting the symmetry properties of the crystal, this integration can then be limited to the symmetry-irreducible wedge of the zone (IBZ). In practice, these integrals are calculated numerically using wavefunctions and eigenvalues at a finite number of **k**-points in the electronic bandstructure of the IBZ. This leads to the so-called *special points method* for Brillouin-zone integration [16, 27, 6], the most commonly used approach for this type of calculations, in which integrations are performed as weighted sums over a grid of representative, or special, **k**-points chosen to yield optimum convergence for smoothly varying functions of **k**. This application of the special points method however proves problematic for the case of metals, where electronic bands intersect the Fermi energy E_f. This leads to discontinuities in the electronic occupation numbers and therefore in the integrands at the Fermi surface, thus yielding slower convergence for a given number of **k**-points. This difficulty can be overcome by the introduction of an artificial temperature-induced and convergence-accelerating broadening of the Fermi surface corresponding to a smoother electron distribution function than the original step function, such as a finite-temperature Fermi distribution. Care must however be taken to ensure that the introduction of such broadening factor does not affect physical quantities of interest.

Once equipped with all the above-mentioned computational models and techniques, a solution to the set of KS equations minimizing the total energy functional of Eq. (26) can be found numerically according to the iterative scheme portrayed in Fig. 32. Any valid solution must be *self-consistent*, meaning that it must be subject to the constraint that the effective KS potential $V^{\sigma}_{KS}(\mathbf{r})$ and the resulting electron density $n(\mathbf{r}, \sigma)$ be consistent with one another, as highlighted in the figure. In practice this is done by successively looping over changes in $V^{\sigma}_{KS}(\mathbf{r})$ and $n(\mathbf{r}, \sigma)$ until the self-consistent agreement is reached.

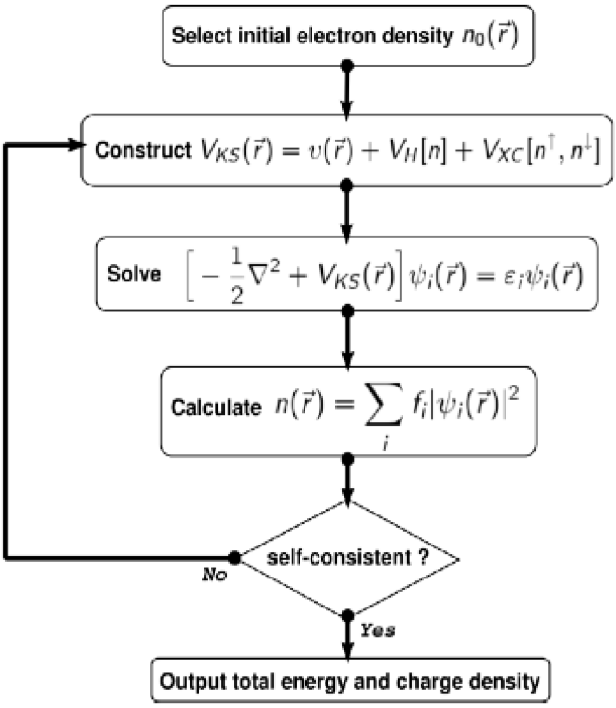

Figure 32: Flow chart illustrating the self-consistent iteration for solving the KS equations. (Figure reproduced from Ref. [71])

B Phonons from Density Functional Perturbation Theory

The starting point in all formulations of Density Functional Perturbation Theory (DFPT), for expanding the DFT method outlined in the previous appendix to systems perturbed away from their equilibrium configurations, is the expansion of the Kohn-Sham (KS) single-particle orbitals, densities and self-consistent potentials in perturbation series of the general form:

$$X(\lambda) = X^{(0)} + \lambda X^{(1)} + \lambda^2 X^{(2)} + \lambda^3 X^{(3)} + ... \tag{45}$$

where $X(\lambda)$ is the quantity of interest and λ is the perturbing parameter. For the case where the quantity of interest is the total energy of the system and where the perturbations consist in atomic displacements away from equilibrium positions, we see that Eq. (45) reduces to a similar expression as the original quadratic form for the expansion of the harmonic potential energy (Eq. (16)), in which $E^{(0)}$ is the total ground-state energy, the $E^{(1)}$ are the atomic forces, the $E^{(2)}$ are the sums of force constants which determine the phonon dispersion curve, and the $E^{(3)}$ represent the cubic anharmonic terms which can be neglected within the harmonic approximation together with all higher-order terms. The theoretical cornerstone underlying DFPT is the so-called $2n+1$ theorem, which asserts that variations of the energy up to order $2n+1$ in a perturbation expansion are determined using only variations in KS orbitals up to order n. Consequently, the atomic forces (the terms of first order in the perturbation expansion of the energy) can be determined directly from the unperturbed ($n = 0$) KS orbitals. This special case of the $2n+1$ theorem for forces is also known as the *Hellmann-Feynman theorem*, and can be proven independently from elementary quantum mechanical perturbation theory. Although the existence of this theorem is not relevant within the context of the linear-response method, it makes DFT codes useful in any computational task relying on the evaluation of atomic forces in crystals, such as the small-displacement method described previously.

As already mentioned, in the context of phonon calculations the main term of interest is $E^{(2)}$, and this can be determined together with the first anharmonic term $E^{(3)}$ from the linear response of the KS orbitals, $\psi^{(1)}$. $\psi^{(1)}$ is given in turn by the solution of the *first-order Sternheimer equation*:

$$\left(H^{(0)} - \varepsilon_i^{(0)}\right)\psi_i^{(1)} = -\left(H^{(1)} - \varepsilon_i^{(1)}\right)\psi_i^{(0)} \tag{46}$$

where i labels the i^{th} solution to the set of KS equations, and $\varepsilon_i^{(0)}$ and $\varepsilon_i^{(1)}$ represent respectively the unperturbed and first order perturbed KS energy eigenvalues for the i^{th} solution to the KS equations. An expression for the first-order variation in the energy eigenvalues $\varepsilon_i^{(1)}$ can be found by imposing the following orthogonalization constraint on the KS orbitals:

$$\left\langle \psi_i^{(0)} \,\middle|\, \psi_i^{(1)} \right\rangle = 0 \tag{47}$$

which gives:

$$\varepsilon_i^{(1)} = \left\langle \psi_i^{(0)} \,\middle|\, H^{(1)} \psi_i^{(0)} \right\rangle \tag{48}$$

Furthermore, $H^{(0)}$ in Eq. (46) represents the unperturbed KS Hamiltonian and $H^{(1)}$ its first-order perturbed variation. In addition to the external perturbing potential $V_{ext}^{(1)}(\mathbf{r})$ induced by the phonon displacement wave traveling through the crystal, $H^{(1)}$ includes also the contributions that $V_{ext}^{(1)}(\mathbf{r})$ makes to the Hartree and Exchange-Correlation potentials due to the perturbations it induces in the electronic charge density of the crystal $n(\mathbf{r})$:

$$H^{(1)}(\mathbf{r}) = V_{ext}^{(1)}(\mathbf{r}) + \int d^3\mathbf{r}' \frac{n^{(1)}(\mathbf{r}')}{|\mathbf{r}-\mathbf{r}'|} + \int d^3\mathbf{r}' \frac{\delta V_{XC}}{\delta n(\mathbf{r}')} n^{(1)}(\mathbf{r}') \tag{49}$$

where $n^{(1)}(\mathbf{r})$ is the first-order variation in the charge density, given in terms of the KS orbitals as:

$$n^{(1)}(\mathbf{r}) = \sum_{i=1}^{N} \left[\left\langle \psi_i^{(1)}(\mathbf{r}) \,\middle|\, \psi_i^{(0)}(\mathbf{r}) \right\rangle + \left\langle \psi_i^{(0)}(\mathbf{r}) \,\middle|\, \psi_i^{(1)}(\mathbf{r}) \right\rangle \right] \tag{50}$$

Moreover, it has been assumed in Eq. (49) that the kinetic energy term in the KS hamiltonian remains unaffected by the external perturbation.

Given the above expressions for $H^{(1)}$ and $\varepsilon_i^{(1)}$, the Sternheimer equation of Eq. (46) can be reduced to a simple linear problem in the plane-wave basis set used for expanding the KS orbitals. Since $H^{(1)}$ depends on $n^{(1)}(\mathbf{r})$, any solution has to be self-consistent in the same sense as explained previously in Section A.3 for the case of the unperturbed ground state KS equations. In particular, the first step in the solution of the linear response problem involves solving self-consistently the unperturbed KS equations to obtain $n^{(0)}(\mathbf{r})$, $\psi_i^{(0)}$ and $\varepsilon_i^{(0)}$. Then, keeping these fixed, Eq. (46) and Eq. (50) are solved iteratively for the first order perturbations in, respectively, the KS orbitals $\psi_i^{(1)}$ and the charge density $n^{(1)}(\mathbf{r})$, until a self-consistent solution is found.

References

[1] G.J. Ackland. High-pressure phases of group-IV, IIIV, and IIVI compounds. *Rep. Prog. Phys.*, 64:483–516, 2001.

[2] G.J. Ackland, M.C. Warren, and S.J. Clark. Practical methods in ab initio lattice dynamics. *J. Phys. Condens. Matter*, 9:7861–7872, 1997.

[3] C.J. Adkins. *Equilibrium Thermodynamics*. Cambridge University Press, 1983.

[4] Dario Alfè. PHON: A program to calculate phonons using the small displacement method. *Comp. Phys. Comm.*, 180(12):2622–2633, 2009.

[5] N.W. Ashcroft and N.D. Mermin. *Solid State Physics*. Saunders College Publishing, 1976.

[6] A. Baldereschi. Mean-Value Point in the Brillouin Zone. *Phys. Rev. B*, 7(12):5212–5215, 1973.

[7] S. Baroni, P. Giannozzi, and A. Testa. Green's-Function Approach to Linear Response in Solids. *Phys. Rev. Lett.*, 58(18):1861–1864, 1987.

[8] S. Baroni, S. Gironcoli, and A. Dal Corso. Phonons and related crystal properties from density-functional perturbation theory. *Rev. Mod. Phys.*, 73(2):515–562, 2001.

[9] P.E. Blochl. Projector augmented-wave method. *Phys. Rev. B*, 50(24):17953–17979, 1994.

[10] F. Bottin. Large-scale ab initio calculations based on three levels of parallelization. *Comp. Mat. Science*, 42(2):329–336, 2008.

[11] E. M. Bringa, J. U. Cazamias, P. Erhart, J. Stlken, N. Tanushev, B. D. Wirth, R. E. Rudd, and M. J. Caturla. Atomistic shock Hugoniot simulation of single-crystal copper. *J. of Appl. Phys.*, 96(7):3793, 2004.

[12] E.M. Bringa, K. Rosolankova, R.E. Rudd, B.A. Remington, J.S. Wark, M. Duchaineau, D.H. Kalantar, J. Hawreliak, and J. Belak. Shock deformation of face-centred-cubic metals on subnanosecond timescales. *Nature materials*, 5(10):805–9, 2006.

[13] J.F. Cannon. Behavior of the Elements at High Pressures. *J. Phys. Chem. Ref. Data*, 3:781–824, 1974.

[14] D.M. Ceperley and B.J. Alder. Ground State of the Electron Gas by a Stochastic Method. *Phys. Rev. Lett.*, 45(7):566–569, 1980.

[15] M. Cerny, M. Sob, J. Pokluda, and P. Sandera. Ab initio calculations of ideal tensile strength and mechanical stability in copper. *J. Phys.: Condens. Matt.*, 16(7):1045–1052, 2004.

[16] D.J. Chadi and M.L. Cohen. Special Points in the Brillouin Zone. *Phys. Rev. B*, 8(12):5747–5753, 1973.

[17] C. Cheng. Uniaxial phase transition in Si: Ab initio calculations. *Phys. Rev. B*, 67(13):1–6, 2003.

[18] D. Clatterbuck, C. Krenn, M. Cohen, and J. Morris. Phonon Instabilities and the Ideal Strength of Aluminum. *Phys. Rev. Lett.*, 91(13):1–4, 2003.

[19] M.L. Cohen. Pseudopotentials and Total Energy Calculations. *Physica Scripta*, T1:5–10, 1982.

[20] M.L. Cohen. Electronic Structure of Solids. *Phys. Rep.*, 6:293–309, 1984.

[21] M.L. Cohen and M.T. Yin. Microscopic Theory of the Phase Transformation and Lattice Dynamics of Si. *Phys. Rev. Lett.*, 45(12):1004–1007, 1980.

[22] A. Dal Corso, A. Pasquarello, and A. Baldereschi. Density-functional perturbation theory for lattice dynamics with ultrasoft pseudopotentials. *Phys. Rev. B*, 56(18):369–372, 1997.

[23] Dal Corso A., A. Pasquarello, A. Baldereschi, and R. Car. Generalized-gradient approximations to density-functional theory: A comparative study for atoms and solids. *Phys. Rev. B*, 53(3):1180–1185, 1996.

[24] R. Dreizler and E. Gross. *Density Functional Theory*. Plenum Press, 1995.

[25] H. G. Drickamer and S. Minomura. Pressure Induced Phase Transitions in Silicon, Germanium and some III-V Compounds. *J. Phys. Chem. Solids*, 23:451–456, 1962.

[26] M. Durandurdu. Diamond to β-Sn phase transition of silicon under hydrostatic and nonhydrostatic compressions. *J. Phys.: Condens. Matt.*, 20(32):325232, 2008.

[27] R.A. Evarestov and V.P. Smirnov. Special points of the brillouin zone and their use in the solid state theory. *Phys. Stat. Sol. (B)*, 119(9):9–40, 1983.

[28] K. Gaál-Nagy. Ab initio study of the enthalpy barriers of the high-pressure phase transition from the cubic-diamond to the $beta;-tin structure of silicon and germanium. *Comp. Mat. Sci.*, 30(1-2):1–7, 2004.

[29] K. Gaál-Nagy, A. Bauer, M. Schmitt, K. Karch, P. Pavone, and D. Strauch. Temperature and Dynamical Effects on the High-Pressure Cubic-Diamond β-Tin Phase Transition in Si and Ge. *Phys. Status Solidi B*, 211(1):275–280, 1999.

[30] K. Gaál-Nagy, P. Pavone, and D. Strauch. Ab initio study of the β-tinImmash phase transitions in silicon and germanium. *Phys. Rev. B*, 69(13):1–11, 2004.

[31] K. Gaál-Nagy and D. Strauch. Transition pressures and enthalpy barriers for the cubic diamondβ-tin transition in Si and Ge under nonhydrostatic conditions. *Phys. Rev. B*, 73(13):1–7, 2006.

[32] T.C. Germann, B.L. Holian, P.S. Lomdahl, and R. Ravelo. Orientation dependence in molecular dynamics simulations of shocked single crystals. *Phys. Rev. Lett.*, 84(23):5351–4, 2000.

[33] P. Giannozzi. QUANTUM ESPRESSO: a modular and open-source software project for quantum simulations of materials. *J. Phys.: Condens. Matt.*, 21(39):395502, 2009.

[34] P. Giannozzi, S. Gironcoli, P. Pavone, and S. Baroni. Ab initio calculation of phonon dispersions in semiconductors. *Phys. Rev. B*, 43(9):7231–7242, 1991.

[35] S.D. Gilev and A.M. Trubachev. Metallization of Monocrystalline Silicon under Shock Compression. *Physica Status Solidi (B)*, 211(1):379–383, 1999.

[36] S. Gironcoli. Lattice dynamics of metals from density-functional perturbation theory. *Phys. Rev. B*, 51(10):6773–6776, 1995.

[37] X. Gonze. A brief introduction to the ABINIT software package. *Zeitschrift für Kristallographie*, 220(5-6-2005):558–562, 2005.

[38] X. Gonze, J. Beuken, R. Caracas, F. Detraux, M. Fuchs, G. Rignanese, L. Sindic, M. Verstraete, G. Zerah, and F. Jollet. First-principles computation of material properties: the ABINIT software project. *Comp. Mat. Science*, 25(3):478–492, 2002.

[39] T. Goto, T. Sato, and Y. Syono. Reduction of Shear Strength and Phase-Transition in Shock-Loaded Silicon. *J. Appl. Phys.*, 21(6):369–371, 1982.

[40] Mool C. Gupta and Arthur L. Ruoff. Static compression of silicon in the [100] and in the [111] directions. *J. Appl. Phys.*, 51(2):1072, 1980.

[41] W.H. Gust and E.B. Royce. Axial Yield Strengths and Two Successive Phase Transition Stressed for Crystalline Silicon. *J. Appl. Phys.*, 42(5):1897–1905, 1971.

[42] D.R. Hamann, M. Schluter, and C. Chiang. Norm-Conserving Pseudopotentials. *Phys. Rev. Lett.*, 43(20):1494–1497, 1979.

[43] C. Hammond. *The Basics of Crystallography and Diffraction.* Oxford Science Publications, 2009.

[44] J. Hawreliak, J. Colvin, J. Eggert, D. Kalantar, H. Lorenzana, J. S. Stölken, H. Davies, T. Germann, B. Holian, K. Kadau, P. Lomdahl, a. Higginbotham, K. Rosolankova, J. Sheppard, and J. Wark. Analysis of the x-ray diffraction signal for the α- transition in shock-compressed iron: Simulation and experiment. *Phys. Rev. B*, 74(18):1–16, 2006.

[45] R. Hennig, A. Wadehra, K. Driver, W. Parker, C. Umrigar, and J. Wilkins. Phase transformation in Si from semiconducting diamond to metallic β-Sn phase in QMC and DFT under hydrostatic and anisotropic stress. *Phys. Rev. B*, 82(1):1–9, 2010.

[46] C. Herring. A New Method for Calculating Wave Functions in Crystals. *Phys. Rev.*, 57:1169–1177, 1940.

[47] P. Hohenberg and W. Kohn. Inhomogeneous Electron Gas. *Phys. Rev.*, 136(3B):864–871, 1964.

[48] B. L. Holian. Plasticity Induced by Shock Waves in Nonequilibrium Molecular-Dynamics Simulations. *Science*, 280(5372):2085–2088, 1998.

[49] W.F. Hosford. *Mechanical Behavior of Materials*. Cambridge University Press, 2005.

[50] J.Z. Hu and I.L. Spain. Phases of Silicon at high pressure. *Solid State Comm.*, 51(5):263–266, 1984.

[51] R. Hull. *Properties of crystalline silicon*. INSPEC, 1999.

[52] J.C. Jamieson. Crystal Structures at High Pressures of Metallic Modifications of Silicon and Germanium. *Science*, 139(3556):762–764, 1963.

[53] R.O. Jones and O. Gunnarsson. The density functional formalsim, its applications and prospects. *Rev. Mod. Phys.*, 61(3):689–746, 1989.

[54] Y.M. Juan and E. Kaxiras. Application of gradient corections to density-functional theory for atoms and solids. *Phys. Rev. B*, 48(20):14944–14952, 1993.

[55] K. Kadau, T. Germann, P. Lomdahl, R. Albers, J.S. Wark, A. Higginbotham, and B. Holian. Shock Waves in Polycrystalline Iron. *Phys. Rev. Lett.*, 98(13):1–4, 2007.

[56] K. Kadau, T.C. Germann, P.S. Lomdahl, and B.L. Holian. Microscopic view of structural phase transitions induced by shock waves. *Science*, 296(5573):1681–4, 2002.

[57] D. Kalantar, J. Belak, G. Collins, J. Colvin, H. Davies, J. Eggert, T. Germann, J. Hawreliak, B. Holian, K. Kadau, P. Lomdahl, H. Lorenzana, M. Meyers, K. Rosolankova, M. Schneider, J. Sheppard, J. Stölken, and J. Wark. Direct Observation of the α-ϵ Transition in Shock-Compressed Iron via Nanosecond X-Ray Diffraction. *Phys. Rev. Lett.*, 95(7):1–4, 2005.

[58] D. Kalantar, G. Collins, J. Colvin, J. Eggert, J. Hawreliak, H. Lorenzana, M. Meyers, R. Minich, K. Rosolankova, and M. Schneider. In situ diffraction measurements of lattice response due to shock loading, including direct observation of the $\alpha\epsilon$ phase transition in iron. *International Journal of Impact Engineering*, 33(1-12):343–352, 2006.

[59] G.I. Kanel, S.V. Razorenov, and V.E. Fortov. *Shock-Wave phenomena and the properties of condensed matter*. Springer, 2004.

[60] G. Kimminau. *Studies of Shock-Induced Plasticity by use of Molecular Dynamics and X-ray Diffraction*. PhD thesis, Oxford University, 2009.

[61] G. Kimminau, P. Erhart, E.M. Bringa, B. Remington, and J.S. Wark. Phonon instabilities in uniaxially compressed fcc metals as seen in molecular dynamics simulations. *Phys. Rev. B*, 81(9):1–4, 2010.

[62] J. Kohanoff. *Electronic Structure Calculations for Solids and Molecules*. Cambridge University Press, 2006.

[63] W. Kohn and L.J. Sham. Self-Consistent Equations Including Exchange and Correlation Effects. *Phys. Rev.*, 140(4A):1133–1138, 1965.

[64] C. Krenn. The non-linear elastic behavior and ideal shear strength of Al and Cu. *Mat. Sci. Eng. A*, 317(1-2):44–48, 2001.

[65] G. Kresse and J. Furthmüller. Efficient iterative schemes for ab initio total-energy calculations using a plane-wave basis set. *Phys. Rev. B*, 54(16):11169–11186, 1996.

[66] G. Kresse, J. Furthmüller, and J. Hafner. Ab initio Force Constant Approach to Phonon Dispersion Relations of Diamond and Graphite. *Europhys. Lett.*, 32(9):729–734, 1995.

[67] G. Kresse and J. Hafner. Norm-conserving and ultrasoft pseudopotentials for first-row and transition elements. *J. Phys.: Condens. Matter*, 6:8245–8257, 1994.

[68] K. Laasonen, A. Pasquarello, R. Car, C. Lee, and D. Vanderbilt. Car-Parinello molecular dynamics with Vanderbilt ultrasoft pseudopotentials. *Phys. Rev. B*, 47(16):10142–10153, 1993.

[69] S. Luo, D. Swift, T. Tierney, D. Paisley, G. Kyrala, R. Johnson, a. Hauer, O. Tschauner, and P. Asimow. Laser-induced shock waves in condensed matter: some techniques and applications. *International Journal of High Pressure Research*, 24(4):409–422, 2004.

[70] N. H. MacMillan. The theoretical strength of solids. *J. Mat. Sci.*, 7(2):239–254, 1972.

[71] R.M. Martin. *Electronic Structure - Basic Theory and Practical Methods.* Cambridge University Press, 2004.

[72] M.I. McMahon and R.J. Nelmes. New high-pressure phase of Si. *Phys. Rev. B*, 47(13):8337–8340, 1993.

[73] M. Methfessel and A.T. Paxton. High-precision sampling for Brillouin-zone integration in metals. *Phys. Rev. B*, 40(6):3616–3621, 1989.

[74] M.A. Meyers. *Dynamic Behavior of Materials.* Wiley, 1994.

[75] M.A. Meyers and K.K. Chawla. *Mechanical behavior of Materials.* Cambridge University Press, second edition, 2009.

[76] Y. Mishin, M. Mehl, D. Papaconstantopoulos, A. Voter, and J. Kress. Structural stability and lattice defects in copper: Ab initio, tight-binding, and embedded-atom calculations. *Phys. Rev. B*, 63(22):1–16, 2001.

[77] N. Moll, M. Bockstedte, M. Fuchs, E. Pehlke, and M. Scheffler. Application of generalized gradient approximations: The diamond-beta tin phase transition in Si and Ge. *Phys. Rev. B*, 52(4):2550–2556, 1995.

[78] H.J. Monkhorst and J.D. Pack. Special points for Brillouin-zone integrations. *Phys. Rev. B*, 13(12):5188–5192, 1976.

[79] A. Mujica, S. Radescu, A. Muñoz, and R. J. Needs. High-Pressure Behaviour of Si AND Ge: A Theoretical Study. *International Journal of High Pressure Research*, 22(2):455–458, 2002.

[80] A. Mujica, A. Rubio, A. Muñoz, and R. Needs. High-pressure phases of group-IV, IIIV, and IIVI compounds. *Rev. Mod. Phys.*, 75(3):863–912, 2003.

[81] S. Narasimhan and S. de Gironcoli. Ab initio calculation of the thermal properties of Cu: Performance of the LDA and GGA. *Phys. Rev. B*, 65(6):1–7, 2002.

[82] R.J. Needs and A. Mujica. First-principles pseudopotential study of the structural phases of silicon. *Phys. Rev. B*, 51(15):9652–9660, 1995.

[83] G. Nilsson and S. Rolandson. Lattice Dynamics of Copper at 80 K. *Phys. Rev. B*, 7(6):2393–2400, 1973.

[84] S. Ogata, J. Li, and S. Yip. Ideal pure shear strength of aluminum and copper. *Science*, 298(5594):807–11, 2002.

[85] H. Olijnyk, S.K. Sikka, and W.B. Holzapfel. Structural Phase Transitions in Si and Ge under Pressures up to 50GPa. *Phys. Lett.*, 10(3):137–140, 1984.

[86] M.C. Payne, M.P. Teter, D.C. Allan, T.A. Arias, and J.D. Joannopoulos. Iterative minimization techniques for ab-initio total-energy calculations: molecular dynamics and conjugate gradients. *Rev. Mod. Phys.*, 64(4):1045–1097, 1992.

[87] J.P. Perdew, K. Burke, and M. Ernzerhof. Generalized Gradient Approximation Made Simple. *Phys. Rev. Lett.*, 77(18):3865–3868, 1996.

[88] J.P. Perdew, K. Burke, and Y. Wang. Generalized gradient approximation for the exchange-correlation hole of a many-electron system. *Phys. Rev. B*, 54(23):533–539, 1996.

[89] J.P. Perdew, J.A. Chevary, S.H. Vosko, K.A. Jackson, M.R. Pederson, D.J. Singh, and C. Fiolhais. Atoms, molecules, solids, and surfaces: Applications of the generalized gradient approximation for exchange and correlation. *Phys. Rev. B*, 46(11):6671–6687, 1992.

[90] J.P. Perdew and W. Yue. Accurate and simple density functional for the electronic exchange energy: Generalized gradient approximation. *Phys. Rev. B*, 33(12):8800–8802, 1986.

[91] J.P. Perdew and A. Zunger. Self-interaction correction to density-functional approximations for many electron systems. *Phys. Rev. B*, 23(10):5048–5079, 1981.

[92] C.J. Pickard. *The planewave pseudopotential method.* In 2nd Kiel workshop on the application of computer simulations to crystallography, Kiel, Germany, 1998.

[93] W.E. Pickett. Pseudopotential methods in Condensed Matter Applications. *Comp. Phys. Rep.*, 9:115, 1989.

[94] S. Plimpton. Fast Parallel Algorithms for Short-Range Molecular Dynamics. *J. Comp. Phys.*, 117:1–19, 1995.

[95] J. Pokluda and P. Sandera. *Micromechanisms of Fracture and Fatigue in a multiscale context.* Springer, 2010.

[96] J. Pokluda, M. Černý, P. Šandera, and M. Šob. Calculations of theoretical strength: State of the art and history. *Journal of Computer-Aided Materials Design*, 11(1):1–28, 2005.

[97] A.M. Rappe, K.M. Rabe, E. Kaxiras, and J.D. Joannopoulos. Optimized pseudopotentials. *Phys. Rev. B*, 41(2):1227–1230, 1990.

[98] K.F. Riley, M.P. Hobson, and S.J. Bence. *Mathematical Methods for Physics and Engineering.* Cambridge University Press, second edition, 2002.

[99] D. Roundy, C. Krenn, M. Cohen, and J. Morris. Ideal Shear Strengths of fcc Aluminum and Copper. *Phys. Rev. Lett.*, 82(13):2713–2716, 1999.

[100] D.S. Sholl and J.A. Steckel. *Density Functional Theory.* Wiley, 2009.

[101] D.J. Singh and L. Nordstrom. *Planewaves, Pseudopotentials, and the LAPW Method.* Springer, 2006.

[102] M. Sob, L.G. Wang, and V. Vitek. Ab Initio calculation of the ideal tensile strength in copper and Nickel Alumide. *Kovove Materialy (Metallic Materials)*, 36(3):145–152, 1998.

[103] M.A. Tschopp and D.L. McDowell. Tension-compression asymmetry in homogeneous dislocation nucleation in single crystal copper. *Appl. Phys. Lett.*, 90(12):121916, 2007.

[104] D. Vanderbilt. Soft self-consistent pseudopotentials in a generalized eigenvalue formalism. *Phys. Rev. B*, 41(11):7892–7895, 1990.

[105] G. Voronin, C. Pantea, T. Zerda, L. Wang, and Y. Zhao. In situ x-ray diffraction study of silicon at pressures up to 15.5 GPa and temperatures up to 1073 K. *Phys. Rev. B*, 68(2):15–18, 2003.

[106] A. Werner, J.A. Sanjurjo, and M. Cardona. X-rays investigation of the alpha to beta phase transition in the GexSi1-x solid solutions at high pressure. *Solid State Comm.*, 44(2):155–158, 1982.

[107] D. Windisch and P. Becker. Silicon lattice parameters as an absolute scale of length for high precision measurements of fundamental constants. *Physica Status Solidi (A)*, 118(2):379–388, 1990.

[108] M.T. Yin and M.L. Cohen. Theory of static structural properties, crystal stability, and phase transformations: Application to Si and Ge. *Phys. Rev. B*, 26(10):5668–5687, 1982.

[109] Y.B. Zel'dovich and Y.P. Raizer. *Physics of shock waves and high-temperature hydrodynamic phenomena.* Academic Press, 1967.